Atomistic simulation of strain relaxation in $In_xGa_{1-x}As$/GaAs quantum dots with nonuniform composition

M. A. Migliorato,[1] A. G. Cullis,[1] M. Fearn,[2] and J. H. Jefferson[2]
[1]Department of Electronic and Electrical Engineering, University of Sheffield, Sheffield S1 3JD, United Kingdom
[2]QinetiQ, Sensors & Electronics Sector, St. Andrews Road, Malvern, Worcs. WR14 3PS, United Kingdom
(Received 22 June 2001; published 27 February 2002)

We report atomistic simulations of $In_xGa_{1-x}As$/GaAs quantum dots (QDs) with nonuniform composition. The Tersoff potential is used to model the atomic interactions of an inhomogeneous system of 400 000 atoms and to obtain dynamic relaxation through energy minimization. From the relaxed atomistic model, the bond deformations are analyzed in order to predict the strain maps. The same technique is also employed to model the strain relaxation of a cleaved QD, allowing us to study the loss of planarity of the cleavage surface and to compare this with experimental scanning tunneling microscopy results. We confirm that an inverted pyramid-like In composition is likely to generate the topographical maps previously reported.

DOI: 10.1103/PhysRevB.65.115316 PACS number(s): 07.05.Tp, 68.37.Ef

INTRODUCTION

Lattice-mismatched heteroepitaxy can give rise to the spontaneous growth of nanometer-sized islands by the Stranski-Krastanow process.[1,2] Because of the predicted strong confinement of carriers, these islands are promising candidates for applications as quantum dots (QDs) in the field of optoelectronic devices. Recently a number of studies[3–6] have tried to reveal the shape and compositions of the islands, as these characteristics are essential for any realistic attempt to calculate electronic properties. As analytic solutions for the strain rely on a large number of approximations, there is increasing interest in simulations. However, the optimum method to be employed, in terms of acceptable accuracy and computer time, is not yet clear. We propose atomistic simulations as this method requires a minimal number of approximations both in the initial atomistic model of the structure and in the methodology employed to extract information, such as local composition and strain.

MODELING ATOMIC INTERACTIONS

To model the atomic interactions, from which displacements may be computed, the empirical potential form proposed by Tersoff[7,8] was used. This allows the total energy of a system of interacting atoms to be described in a very convenient functional form that preserves both the characteristics of a pair potential and a strong dependence of bond order upon the local environment, thus effectively incorporating the structural chemistry of covalent systems. The functional form can be written as

$$E=\frac{1}{2}\sum_{j\neq i} f_c(r_{ij})[V_R(r_{ij})+b_{ij}V_A(r_{ij})], \tag{1}$$

where V_R and V_A are the repulsive and attractive parts of the potential, essentially Morse-like pair potentials. These are functions of four material-dependent parameters (A, B, λ_{ij}, μ_{ij}), and f_c is a cutoff function (dependent on two further parameters R and S) that reduces the number of neighbors of atom i that contribute to the total energy. In Eq. (1), b_{ij} represents the bond order and can be expressed as

$$b_{ij}=[1+(\beta_i\zeta_{ij})^{n_i}]^{-n_i/2} \tag{2}$$

where

$$\zeta_{ij}=\sum_{k\neq i,j} f_c(r_{ik})g(\theta_{ijk})\exp[\lambda^3(r_{ij}-r_{ik})^3]. \tag{3}$$

It is clear that b_{ij} depends upon parameters β_i, n_i, and λ. The latter, contained within the exponential factor in Eq. (3), was introduced as a refinement of the original formulation by Sayed *et al.*[9] in order to reduce the unrealistically large influence of distant neighbors on immediate bonds. The function $g(\theta_{ijk})$ is dependent upon the angle between bonds ij and ik and three parameters c, d, and h. This formulation is, therefore, based upon a set of independent parameters that are different not only for different materials but specific to the type of bond. The ternary alloy $In_xGa_{1-x}As$ needs a further set of parameters in addition to those needed for InAs and GaAs alone, i.e., the set of parameters for the In-Ga interaction. This set was obtained through an averaging scheme first proposed by Tersoff[8] and utilized by Ashu *et al.*[10] for $In_{0.5}Ga_{0.5}As$.

An extensive study of the validity and transferability of the potential when applied to silicon and germanium was described by Tersoff when the functional form was first introduced,[7,8] while the same model has been applied to AlAs,[9] InAs,[10] and GaAs.[11] We have improved the parameter fit for InAs of Ashu *et al.*[10] since this overestimates the cohesive energy [3.56 eV instead of the experimental value of 3.1 eV (Ref. 12)] and underestimates slightly the lattice constant [5.975 Å instead of 6.058 Å (Ref. 13)]. We were then able to test the validity of the parameter sets on the ternary alloy $In_xGa_{1-x}As$ and investigate the portability of the method to more inhomogeneous situations than the bulk III-V semiconductors. Following the method used in Smith,[11] we fitted our set of parameters to four experimental quantities: cohesive energy (E_{coh}), lattice constant (a), bulk modulus (B), and shear constant (C'). Of the three sets of

 ©2002 The American Physical Society

TABLE I. Parameters for InAs used in the model potential, Eqs. (1)–(3).

In-As parameters	
A	2291.292969
B	424.874512
λ_{ij}	2.517917
μ_{ij}	1.678611
c	0.9989
d	0.82608
h	−0.5145
n	7.141472
β	0.3779
λ	1.5
R	3.6
S	3.8

parameters needed, we only refitted the set for In-As (Table I), using directly the In-In fit of Ashu *et al.*[10] and the As-As fit of Smith.[11] The choice of R and S for the cutoff function was made in order to include the effects of the contributions of at least second nearest neighbors to the total energy. The predictions obtained with the refitted parameters, as shown in Table II, are seen to agree accurately with the experimental values. The elastic constant c_{44}, not included in the fitting process, is also found to be in good agreement (0.417 Mbar) with experiment [0.396 MBar (Ref. 13)]. Using our refitted parameters for In-As and the parameters for GaAs fitted by Sayed *et al.*,[9] we then tested the transferability of the method to $In_xGa_{1-x}As$, studying the behavior of the cohesive energy and the average lattice constant for three different values of x, compared with the values predicted with Vegard's law. Results (Table III) from the simulations implemented with the OXON code[14] on a zinc-blende supercell were satisfactory with the differences between the experimental and computed values being less than 1%. This gives us confidence that the model is sufficiently accurate to be applied to inhomogeneous structures on the nanoscale, including quantum wells and QDs.

ATOMISTIC MODEL OF A QD

The structural studies realized in recent years have suggested that $In_xGa_{1-x}As/GaAs$ QDs can be either lens

TABLE II. Comparison between the experimental values, the calculated values obtained using the parameters fitted by Ref. 10, and those obtained using our fitted parameters. The experimental values were all derived from Ref. 13, apart from (a) which was obtained from Ref. 12.

	Experiment	Using parameters from Ref. 10	Refitted
E_{coh} (eV)	−3.10[a]	−3.567	−3.10
a (E)	6.058	5.975	6.058
B (Mbar)	0.579	0.600	0.580
C' (Mbar)	0.190	0.204	0.190

TABLE III. Comparison between values for cohesive energy and lattice constant calculated values obtained using our fitted parameters for three different compositions of $In_xGa_{1-x}As$.

	25% indium	50% indium	75% indium
E_{coh} (eV)	−3.20 (-3.21)	−3.16 (−3.18)	−3.13 (−3.14)
a (E)	5.779 (5.754)	5.865 (5.856)	5.970 (5.957)

shaped[5,6] or truncated pyramids,[15–18] and more recently nonuniformities in composition have been investigated, revealing a higher concentration of In near the top of the pyramid compared to the bottom.[3–5] Following these observations we decided to study truncated pyramidal QDs, 7 nm high and 16 nm wide, with base edges aligned along the [100] and [010] directions and including rounded sloping edges to eliminate unphysically sharp features. The facets form an angle of 50° with the (001) plane and a rounded top is added, consistent with experimental observations such as those reported by Zou *et al.*[6] A nonuniform composition similar to the inverted pyramid first proposed by Liu *et al.*[3] was also used, although we introduced a "trumpet-shaped" graded composition [Fig. 2(a)], since this is consistent with initial QD nucleation from a high-concentration alloy, together with the overall In distribution found in Walther *et al.*[4] The higher In concentration at the top of the QD is a result of the strain-determined chemical potential gradients driving surface diffusion of adatoms during growth. Compared to models consisting of a simple gradient of composition increasing from bottom to top, an inverted pyramid or trumpet shape also allows regions with high In concentration to be more directly in contact with the wetting layer, reducing the potential barriers between electron and hole bands of the wetting layer and the QD. This is in accord with experimental observations,[19,20] which show high efficiency of carrier transport from the wetting layer into the QDs. In the present work, for reasonable consistency with the growth conditions of Liu *et al.*[3] ($In_{0.5}Ga_{0.5}As$ on GaAs), we choose a fixed 50% In concentration for the wetting layer and a graded composition ranging from 30% In at the bottom of the pyramid to 80% at the top, so as to give a partial intermixing of Ga and In throughout the QD. The relatively abrupt change in composition between the wetting layer and the QD results from the fact that the former forms first (with a composition gradient due to the action of segregation) and is later overgrown by the QD (with its own inhomogeneous composition distribution).

Using these specifications for the structure and composition, and using simple elastic theory, we were able to construct, using ~200 000 atoms, an atomistic model of the QD, shown uncapped in Fig. 1, with atoms located near to their equilibrium positions after relaxation. For these simulations In and Ga atoms were randomly assigned to their atomic sites in an uncorrelated way (δ correlated), according to the compositional profile previously discussed, thus creating a compositional disorder that reproduces stochastically the experimental condition. The subsequent step, which was to cover the QD with a further ~200 000 atoms to form a capping layer, was not trivial since controlled bending of the

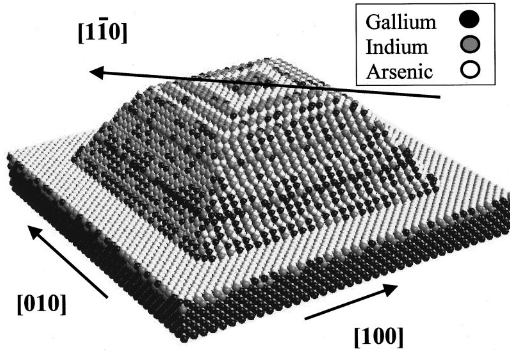

FIG. 1. Atomistic model of an $In_xGa_{1-x}As$ QD. The QD is shown uncapped and lying on a 2 ML wetting layer with 50% In composition, and a pure GaAs substrate.

{001} lattice planes had to be introduced to prevent the structure from forming dislocation lines extending into the capping layers in a nonphysical manner. Compression in the [001] direction of growth of the top layers of the QD and of the capping layers immediately on top of these, together with an expansion of the lattice planes in the proximity of the side facets, was clearly necessary in order to accommodate the atoms without creating misfit dislocations. Once the capping layer was applied on top of the pyramid the simulation box dimensions were 23×23×17 nm, containing a total of ~400 000 atoms. Rigid boundaries were subsequently applied on the six surfaces of the box. The choice of rigid boundaries, as opposed to periodic, was made to circumvent problems connected with propagation of the perpendicular strain outside the simulation box. The use of rigid boundaries is also slightly more efficient in terms of computer memory.

The resulting dislocation-free structure was relaxed using the steepest descent technique within the OXON code[14] and strain information was then obtained directly from the atomic-bond deformations, taking into account the local composition of the material.

In order to evaluate the diagonal components of the strain tensor we used elastic theory. According to Singh,[21] one can relate the vectors defining the unit cell in the unstrained and strained case through the set relations

$$x' = (1+\varepsilon_{xx})\hat{x} + \varepsilon_{xy}\hat{y} + \varepsilon_{xz}\hat{z},$$

$$y' = \varepsilon_{yx}\hat{x} + (1+\varepsilon_{yy})\hat{y} + \varepsilon_{yz}\hat{z},$$

$$z' = \varepsilon_{zx}x' + \varepsilon_{zy}\hat{y} + (1+\varepsilon_{zz})\hat{z}, \tag{4}$$

where $\hat{\mathbf{x}}$, $\hat{\mathbf{y}}$, and $\hat{\mathbf{z}}$ are orthogonal unit vectors of the unstrained system and $\mathbf{x}'$, $\mathbf{y}'$, and $\mathbf{z}'$ are the (generally nonorthogonal) vectors after a distortion with components ε_{ij} is applied to the unit cell. The diagonal components of this distortion are equal to the diagonal components of the stain tensor. They relate to deviations from an effective bulk material of uniform composition, obtained by averaging over all atoms up to third-neighbor distance from the atom under investigation. This procedure allows us to resolve composition fluctuations on the atomic scale while still enabling the influence of the environment on local elastic properties to be determined.

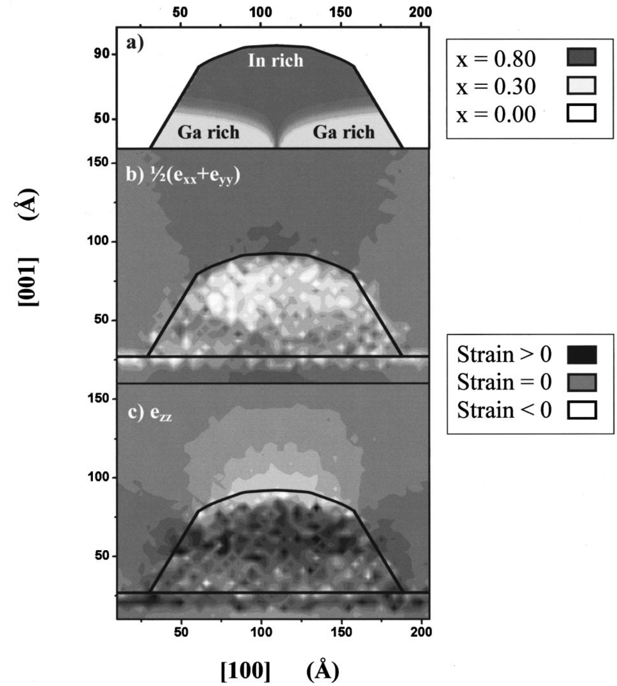

FIG. 2. (a) Simulated [100] cross section of the QD showing a trumpet-shaped In composition distribution. The darker regions are In rich, while the brighter are Ga rich. (b) Simulated [100] cross section of the QD parallel component of the strain. The In-rich regions are highly strained. Positive values of the parallel strain are found at the top of the pyramid and in the capping layer above it. (c) [100] QD perpendicular component of the strain cross-section map: positive values of the perpendicular strain are found outside the QD.

RESULTS I: STRAIN MAPS

Presented in Figs. 2(b) and 2(c) are the maps of the average diagonal component of the strain in the growth plane (parallel) and its diagonal component in the direction of growth (perpendicular) in a (100) plane passing through the center of the QD. The same maps in a (110) plane parallel to the main diagonal of the QD base are shown instead in Figs. 3(a) and 3(b). The darker (brighter) regions represent larger positive (negative) strain, i.e., an expansion (compression) of the lattice constant. The effect of plane bending inside the QD and in the capping layer is clearly visible, as a lighter region for the perpendicular strain and a darker region for the parallel strain appearing at the top of the QD and extending for a large distance into the capping layer.

In Fig. 2(b) we see that there is an abrupt change in sign of the xx and yy strain components as we pass through the In-rich region near the top of the dot into the GaAs cap. This simply reflects the compressive strain in the dot and the expansive strain in the cap, while the inverse (i.e., expansive strain in the dot and compressive strain in the cap) applies for the zz component of strain [Fig. 2(c)] in order to (ap-

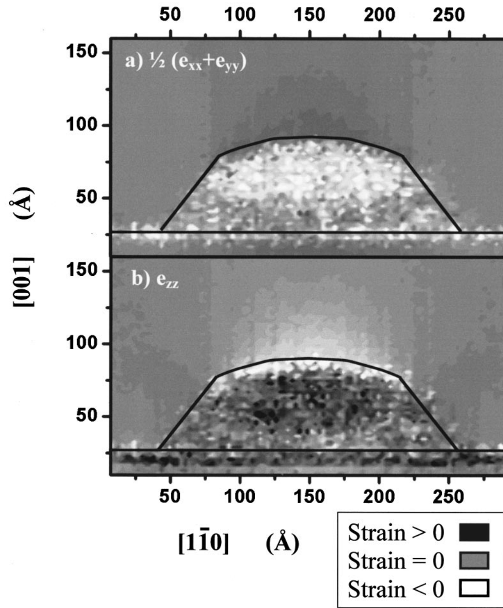

FIG. 3. Simulated $[1\bar{1}0]$ cross section of the QD (a) parallel strain and (b) perpendicular strain.

proximately) maintain Poisson's ratio. However, a more subtle effect seen in Fig. 2 is that of compressive strain for all strain components over a narrow region inside the dot near the dot-cap interface. This is a consequence of the dome-shaped geometry of the dot, which ensures that the In-rich region just below the interface feels compressive forces in all directions. We have confirmed that this is indeed a geometrical effect by performing simulations on flat-topped dots for which the zz strain components are always expansive inside the dot.

In contrast to the strain variation near the top of the dot, the perpendicular strain in the regions near the side facets remains expansive as we pass from dot to cap, though there is an abrupt change in its magnitude. As explained above, the expansion of the dot in the perpendicular direction is a consequence of the compression in the parallel direction, approximately preserving Poisson's ratio. Hence the GaAs in the cap adjacent to the side facets must also be under expansive strain vertically, as shown in Fig. 2(c). This in turn gives rise to a weakly compressive parallel strain for the GaAs [Fig. 2(b)].

The maximum positive (negative) values of the perpendicular (parallel) component of the strain are found in the center of the QD, as expected, due to the presence of the In-rich region.

The parallel strain ranges from 3% at the top of the pyramid and in the capping layer immediately above it to -5% in the indium-rich region in the center of the pyramid, while the perpendicular strain ranges from a minimum of -7% in the capping layer to a large 9% at the top of the pyramid. While the compression of the In rich regions in the plane (-5%) is directly comparable with the lattice mismatch between an In-rich InGaAs alloy and GaAs, the maximum perpendicular strain is higher than the 7.5% that simple elastic theory would predict if layers of InAs were deposited

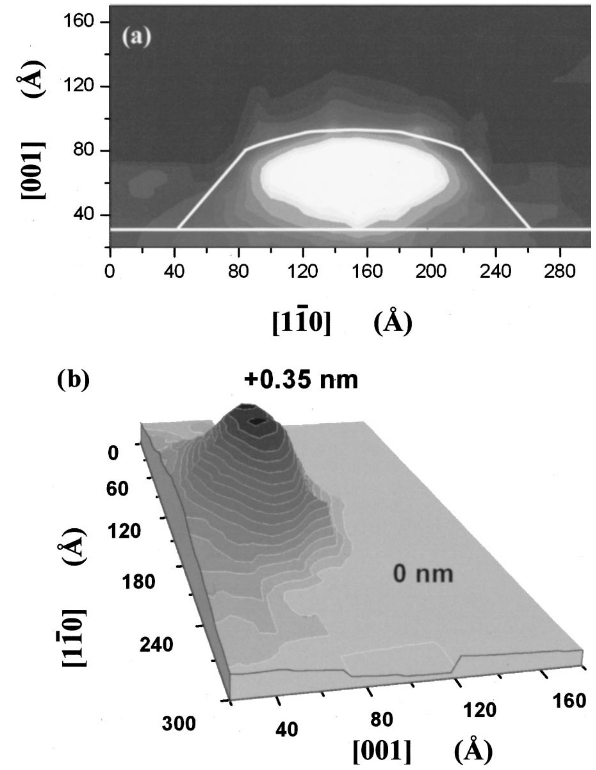

FIG. 4. (a) 2D topographical map of the (110) cleavage plane. The highly strained regions undergo relaxation when the sample is cleaved and emerge from the background (brighter regions). (b) 3D topographical map showing that the maximum calculated height of the relaxed region is 0.35 nm above the cleavage plane.

pseudomorphically on a GaAs substrate. This result is caused by the presence of alloy fluctuations in the nominal 80% In-rich InGaAs alloy at the top of the pyramid. This causes neighboring regions to have different contents of In and therefore different strain states: local regions with smaller In contents, but neighbored with regions of higher In content, will be forced into a state of higher strain than the one predicted by elastic theory.

RESULTS II: SURFACE RELAXATION

In order to demonstrate the strain relaxation on the open surface of a cleaved QD, the atomistic model was subsequently cleaved about one of its base diagonals, the $[1\bar{1}0]$ direction (leaving a total number of ~200 000 atoms), and was then allowed to relax using the OXON code. The result of the simulation is presented in the form of a topographical map of the open boundary surface, i.e., the cleavage plane, in two dimensions (2D) and 3D [Figs. 4(a) and 4(b)]. As expected the regions with higher strain, i.e., the regions with the higher concentration of In, relax along the direction [110], orthogonal to the cleavage plane, resulting in a strong loss of planarity of the cleaved surface. The topographical map is remarkably similar to the experimental topographical picture obtained using the scanning tunneling microscopy (STM) technique, presented in Fig. 1(b) of Liu *et al.*,[3] which was justified by proposing an inverted pyramid-like In distri-

bution. The predicted distortion of the cleavage plane is $\sim$0.35 nm, in close agreement with the $\sim$0.3 nm distortion measured experimentally.[3] Indeed, the closeness between the predicted and measured distortions implies that the effect of outward strain relaxation upon the STM image was much more substantial than purely electronic effects. In addition, in both the experiment[3] and our calculations the wetting layer does not undergo an appreciable relaxation, this being due to its small dimensions ($\sim$2 ML) and the 50% In composition that results in a lattice mismatch with GaAs of $\sim$3.5%, considerably reducing the strain.

CONCLUSIONS

In conclusion, it is clear that our work strongly supports the model proposed by Liu *et al.*,[3] at least in the essential concept of a composition distribution that not only includes a higher concentration of In in the top of the QD, but also in the core of the truncated pyramid. As pointed out above, this particular In distribution can be accounted for by considering the chemical potential gradients which exist at the side of a quantum dot during growth. Further refinements to the atomistic model are possible, though our proposed trumpet-shaped composition distribution results in the topographical map of a cleaved QD statistically similar to that presented in Liu *et al.*[3] In general terms, we have demonstrated that atomistic simulations accurately reproduce the strain pattern of QDs, with minimal approximations, offering a valid and improved alternative to continuum elasticity theory and a useful tool with which to investigate reliably the consequences of compositional variations in semiconductor nanostructures.

ACKNOWLEDGMENTS

The authors would like to thank Dr. Andrew Horsfield for supplying a version of the OXON atomistic modeling code. M.F. and J.H.J. acknowledge the support of the U.K. Ministry of Defense.

[1] S. Guha, A. Madhukar, and K.C. Rajkumar, Appl. Phys. Lett. **57**, 2110 (1990).
[2] R. Nötzel, Semicond. Sci. Technol. **11**, 136 (1996).
[3] N. Liu, J. Tersoff, O. Baklenov, A.L. Holmes, Jr., and C.K. Shih, Phys. Rev. Lett. **84**, 334 (2000).
[4] T. Walther, A.G. Cullis, D.J. Norris, and M. Hopkinson, Phys. Rev. Lett. **86**, 2381 (2001).
[5] I. Kegel, T.H. Metzger, A. Lorke, J. Peisl, J. Stangl, G. Bauer, J.M. García, and P.M. Petroff, Phys. Rev. Lett. **85**, 1694 (2000).
[6] J. Zou, X.Z. Liao, D.J.H. Cockayne, and R. Leon, Phys. Rev. B **59**, 12 279 (1999).
[7] J. Tersoff, Phys. Rev. Lett. **56**, 632 (1986).
[8] J. Tersoff, Phys. Rev. B **39**, 5566 (1989).
[9] M. Sayed, J.H. Jefferson, A.B. Walker, and A.G. Cullis, Nucl. Instrum. Methods Phys. Res. B **102**, 218 (1995).
[10] P.A. Ashu, J.H. Jefferson, A.G. Cullis, W.E. Hagston, and C.R. Whitehouse, J. Cryst. Growth **150**, 176 (1995).
[11] R. Smith, Nucl. Instrum. Methods Phys. Res. B **67**, 335 (1992).
[12] W.A. Harrison, *Electronic Structure and Properties of Solids* (Freeman, San Francisco, 1980).
[13] *Semiconductors—Basic Data*, 2nd ed., edited by O. Madelung (Springer, Berlin, (1996).
[14] The OXON software is an $O(N)$ tight-binding-based program owned and distributed by the Department of Materials at Oxford University. In the present work, this code was used to perform, in an efficient manner, dynamic energy relaxation within the Tersoff model and, consequently, determine the atomic displacements.
[15] J-Y. Marzin, J.M. Gérard, A. Izraël, D. Barrier, and G. Bastard, Phys. Rev. Lett. **73**, 716 (1994).
[16] R. Heitz, M. Grundmann, N.N. Ledentsov, L. Heckey, M. Veit, D. Bimberg, V.M. Ustinov, A.Yu. Egorov, E. Zhuckov, P.S. Kop'ev, and Zh.I. Alferov, Appl. Phys. Lett. **68**, 361 (1996).
[17] M. Grundmann, N.N. Ledentsov, O. Stier, D. Bimberg, V.M. Ustinov, P.S. Kop'ev, and Zh.I. Alferov, Appl. Phys. Lett. **68**, 979 (1996).
[18] H. Lee, R. Lowe-Webb, W. Yang, and P.C. Sercel, Appl. Phys. Lett. **72**, 812 (1998).
[19] B. Ohnesorge, M. Albrecht, J. Oshinowo, A. Forchel, and Y. Arakawa, Phys. Rev. B **54**, 11 532 (1996).
[20] R. Heitz, M. Veit, N.N. Ledentsov, A. Hoffmann, D. Bimberg, V.M. Ustinov, P.S. Kop'ev, and Zh.I. Alferov, Phys. Rev. B **56**, 10 435 (1997).
[21] J. Singh, *Physics of Semiconductors and their Heterostructures* (McGraw-Hill, New York, 1993).